Journal of Materials Chemistry A

Emerging Nanostructured Carbon-based Non-precious Metal Electrocatalysts for Selectively Electrochemical CO2 Reduction to CO

Journal:	*Journal of Materials Chemistry A*
Manuscript ID	TA-REV-09-2019-009681.R1
Article Type:	Review Article
Date Submitted by the Author:	08-Oct-2019
Complete List of Authors:	Wang, Xinyue; Zhejiang University Zhao, Qidong; Dalian University of Technology, Environmental Science and Technology Yang, Bin; Zhejiang University, Li, Zhongjian; Zhejiang University, Bo, Zheng; Zhejiang University, Department of Energy Engineering Lam, Kwok-ho; The Hong Kong Polytechnic University Adli, Nadia; Department of Chemical and Biological Engineering, University at Buffalo, The State University of New York lei, lecheng; Zhejiang University Wen, Zhenhai; Chinese Academy of Sciences, Fujian Institute of Research on the Structure of Matter Wu, Gang; University at Buffalo, SUNY, Chemical and Biological Engineering Hou, Yang; Zhejiang University

REVIEW

Emerging Nanostructured Carbon-based Non-precious Metal Electrocatalysts for Selectively Electrochemical CO_2 Reduction to CO

Received 00th January 20xx,
Accepted 00th January 20xx

DOI: 10.1039/x0xx00000x

Xinyue Wang,[a] Qidong Zhao,[c] Bin Yang,[a] Zhongjian Li,[a] Zheng Bo,[d] Kwok Ho Lam,[e] Nadia Mohd Adli,[f] Lecheng Lei,[a] Zhenhai Wen,[b] * Gang Wu,[f] * and Yang Hou,[a] *

Electrochemical carbon dioxide (CO_2) reduction (ECR) represents one of the most promising technologies for CO_2 conversion into value-added feedstock from carbon monoxide (CO) to a variety of hydrocarbons. As the raw material for Fischer-Tropsch synthesis, CO is one of the most desirable ECR products and has recently received extensive research attentions. Although noble metal based materials, such as Au and Ag, show high selectivity towards conversion CO_2 to CO, their relatively scarce and high cost seriously limit practical commercial applications. Nanostructured carbon-based non-precious metal electrocatalysts (Nano-CNMs) are of tremendous interest in the fields of ECR catalysis due to their tunable structures and electronic properties. Herein, we present an overview of recent progress in the application of the Nano-CNMs, mainly including heteroatoms-doped carbon, transition metal-heteroatoms complex doped carbon, and carbon-based hybrid materials, with emphasis on electrocatalytic conversion of CO_2 to CO. We particularly focus on discussing the structure/composition-performance relationships with regard to electronic structure, surface property, doping content, and associated electrocatalytic performance in various Nano-CNMs. We finally outline the promising future research directions in the development of high-selectivity ECR electrocatalysts for CO production and the stringent challenges in fundamental research and the feasibility for industrial applications.

1. Introduction

Conversion of carbon dioxide (CO_2) into value-added fuels or chemicals holds great promise for reducing CO_2 emissions and facilitating the storage of renewable energy.[1] Compared with traditional CO_2 conversion methods, electrochemical CO_2 reduction (ECR) technology driven by renewable energy sources of electricity has been widely recognized as a promising path owing to its multiple advantages, including: (I) mild operating conditions, (II) tunable conversion efficiency and selectivity by applied voltage or current, and (III) potential integration into energy storage systems as a unit.[2-4]

As a means of energy conversion and storage, ECR is a promising strategy to convert CO_2 into desirable chemical fuels, including carbon monoxide (CO), methane, ethylene, and ethane, *etc.* for energy storage. In particular, CO gas is widely utilized as an essential raw material for Fischer-Tropsch synthesis in industrial production and also as reducing agent during metallurgical process.[5] Compared with the multi-electron reduction reactions forming methane or ethylene products, the formation of CO molecules involves two-electron transfer process that significantly reduces the ECR reaction barriers and the conversion mechanism is relatively clear.[6] As a result, the ECR to CO has been widely studied in the past years, and it is generally accepted that the electrochemical CO_2-to-CO conversion involves the following four crucial steps:[7-10]

$CO_2 + * = *CO_2$ (I)

$*CO_2 + H^+ + e^- = *COOH$ (II)

$*COOH + H^+ + e^- = *CO + H_2O$ (III)

$*CO = CO + *$ (IV)

Theoretical calculations demonstrate that electrocatalysts are the key components for CO_2-to-CO conversion because they not only function to better stabilize *COOH intermediates and to enhance the electron transport, but also play a paramount role in converting *COOH into *CO. Meanwhile, a balanced adsorption/desorption capability in the ECR electrocatalyst is of crucial importance to promote CO production. In these regards, design and development of high-performance ECR electrocatalysts for selective CO production should take these points into consideration. Up to now, various precious metal catalysts, such as Au and Ag based materials with high activity and selectivity,[11-13] have been extensively studied as electrocatalysts towards CO production.[12, 14-16] Unfortunately, high price and scarcity of these precious metal electrocatalysts hinder large-scale practical productions. In recent years, non-precious metal catalysts, such as alloy, transition metal compounds, and transition metal-based molecular catalysts,[17] have been widely

[a] Key Laboratory of Biomass Chemical Engineering of Ministry of Education, College of Chemical and Biological Engineering, Zhejiang University, Hangzhou 310027, China. Email: yhou@zju.edu.cn.
[b] CAS Key Laboratory of Design and Assembly of Functional Nanostructures, and Fujian Provincial Key Laboratory of Nanomaterials, Fujian Institute of Research on the Structure of Matter, Chinese Academy of Sciences, Fuzhou, China. Email: wen@fjirsm.ac.cn.
[c] School of Petroleum and Chemical Engineering, Dalian University of Technology, Panjin Campus, NO.2 Dagong Road, New District of Liaodong Bay, Panjin 124221, Liaoning Province, China.
[d] State Key Laboratory of Clean Energy Utilization, College of Energy Engineering, Zhejiang University Hangzhou, China.
[e] Department of Electrical Engineering, The Hong Kong Polytechnic University, Hunghom, Hong Kong.
[f] Department of Chemical and Biological Engineering, University at Buffalo, the State University of New York, Buffalo, NY, 14260, United States. Email: gangwu@buffalo.edu.

reported to replace precious metal materials to realize CO_2-to-CO conversion. For practical ECR applications, essential requirements of high activity and selectivity, low cost, and high stability should be considered. Despite non-precious metal ECR electrocatalysts overcoming the price constraints, they can hardly meet at least one or more of the aforementioned requirements.[18, 19] Recently, nanostructured carbon-based non-precious metal electrocatalysts (Nano-CNMs) have received extensive attention owing to their low cost, excellent stability, and controllability, allowing for their use as supports for active materials and compositions tuning, as well as morphology and structure fine-tuning to efficiently catalyze the reactions. The emergence of a large number of novel Nano-CNMs with excellent ECR performance has prompted us to review this emerging research field. To the best of our knowledge, although several excellent works have summarized the recent advances in carbon-based electrocatalysts for ECR, comprehensive reviews on Nano-CNMs for CO_2-to-CO conversion *via* ECR remain missing.

In this review, we will summarize the recent development of Nano-CNMs materials, and mainly focus on their relationships between electrocatalytic performance and structure/composition. Based on the structural features, the content can be divided into three sections: metal-free heteroatoms-doped carbon materials, transition metal-heteroatoms complex doped carbon materials, and carbon-based hybrid materials. The synthesis methods and corresponding ECR performances of these Nano-CNMs materials are summarized in Table 1 and Table 2. Finally, future opportunities and challenges of Nano-CNMs materials for highly efficient CO production *via* ECR will be highlighted.

2. Metal-free heteroatoms-doped carbon materials

Zhenhai Wen received his M.Sc. from Beijing University of Technology in 2004 and Ph.D. degree from the Chinese Academy of Sciences China in 2008. Then he worked in Max Planck Institute for Polymer Research in Germany as Humboldt postdoctoral research scholar and then moved to University of Wisconsin-Milwaukee as a postdoctoral researcher in 2010. He joined the Fujian Institute of Research on the Structure of Matter, Chinese Academy of Sciences since 2015. Research topics mainly include the design and synthesis of functional nanostructures and exploration their applications in electrochemical energy conversion and storage system.

Gang Wu is an associate professor in the Department of Chemical and Biological Engineering at the University at Buffalo (USA). He completed his Ph.D. studies at the Harbin Institute of Technology (China) in 2004 followed by postdoctoral trainings at Tsinghua University (China; 2004-2006), the University of South Carolina (USA; 2006-2008), and Los Alamos National Laboratory (LANL, USA; 2008-2010). Then he was promoted being a staff scientist at LANL until joining the University of Buffalo (USA) in 2014. He was promoted to a tenured professor in 2018. His research focuses on functional materials and catalysts for electrochemical energy storage and conversion.

Yang Hou received his Ph.D degree from the School of Environmental Science & Technology of Dalian University of Technology in 2011, and then did ~6 years of postdoctoral research in the Department of Chemistry at the University of California, Riverside, Department of Mechanical Engineering, University of Wisconsin–Milwaukee, and Center for Advancing Electronics Dresden, Technische Universität Dresden. He has been a Professor in College of Chemical and Biological Engineering at Zhejiang University since March 2017. His current research focuses on the design and synthesis of low-dimensional nanomaterials for energy and environmental applications.

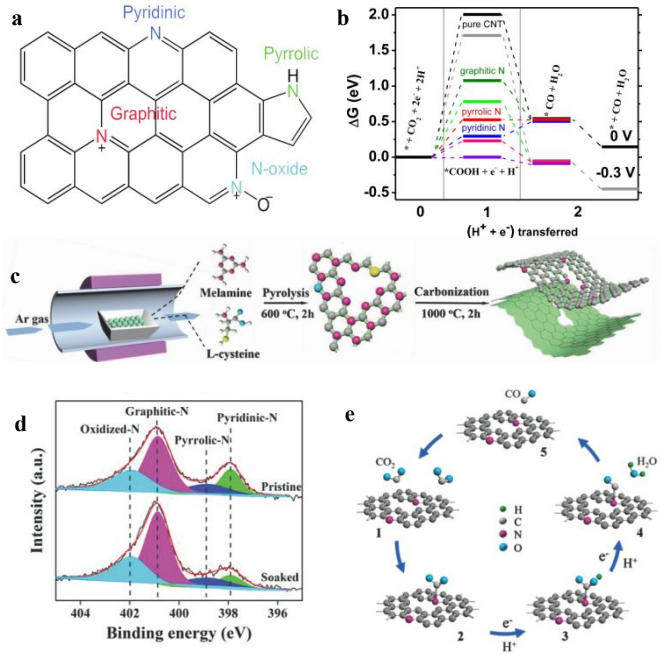

Figure 1. (a) Schematic illustration of NG. Reproduced with permission from ref. 20, Copyright 2017, Elsevier Ltd. (b) Calculated free energy diagram of ECR for CO production on pristine CNTs and NCNTs. Reproduced with permission from ref. 21, Copyright 2015, American Chemical Society. (c) Schematic diagram of synthesis processes for N-GRW. (d) High-revolution N 1s XPS spectra of N-GRW before and after being soaked in 1 M H_3PO_4 solution. (e) Schematic diagram of reaction mechanism for ECR on N-GRW. Reproduced with permission from ref. 22, Copyright 2018, Wiley-VCH.

In the last few years, heteroatoms-doped carbon materials, such as, nitrogen (N) doped, fluorine (F) doped, sulfur (S) doped, and boron (B) doped nanocarbons, have been widely developed as efficient electrocatalysts for ECR, and great progress have been made.[23] Although those reported heteroatoms-doped carbon materials are metal-free catalysts, their catalytic activities could compete well with those of the precious metal containing materials. The nature of outstanding ECR electrocatalytic activity can be attributed to the introduction of heteroatoms, result in conjugating sp^2-sp^2 linkages or the delocalization of π-orbital electron.[24] Benefiting from the different electronegativity of heteroatoms (N, B, and F, *etc*.) with carbon atoms, the introduced heteroatoms could disrupt the lattice arrangement of carbon and produce positive or negative groups, such as B-C bonds and N-C bonds, which can interact with CO_2 or *COOH intermediates, thus reducing the energy barrier of the reaction and driving the ECR reaction.[25] In light of these benefits, numerous heteroatoms-doped nanocarbon electrocatalysts have been developed to produce CO *via* ECR.

2.1. Metal-free N-doped carbon materials

Among well-developed heteroatoms-doped carbon materials, N-doped nanocarbon materials are considered as ideal ECR electrocatalysts for CO production, owing to their good selectivity and stability.[26] Density functional theory (DFT) calculations illustrated that the N dopants could change the spin density of adjacent carbon atoms and induce a higher density of donor states close to the Fermi level, which could lead to the increased electron transfer rate of N-doped nanocarbons.[27] The similar size of N atoms with C atoms resulted in the fact that the C atoms were easily replaced by N atoms. According to the different chemical environments of N atoms, the N dopants were divided into four forms, pyridinic-N, graphitic-N, pyrrolic-N, and oxidized-N, as shown in Figure 1a.[20] Although most previous studies demonstrated that the pyridinic-N contributed to the high ECR activities due to its positive effect on the rate-determining step,[21, 28, 29] there was still a debate for the role of pyridinic-N and pyrrolic-N in ECR catalysis. For instance, a based pyrrolic-N doped carbon-wrapped carbon nanotubes (CN-H-CNTs) was prepared by a hydrothermal steam etching strategy.[30] X-ray photoelectron spectroscopy (XPS) results showed that the pyridinic-N could be partially removed while the percentage of pyrrolic-N would accordingly increase by the etching treatment; as a result, the CN-H-CNTs showed an increased CO Faradaic efficiency (FE) from 60% to 88% for ECR. The reporters also believed that the presence of pyrrolic-N greatly inhibited the competitive reaction of water splitting.

Besides this etching strategy, alternative effective synthesis methods have been developed to regulate the type of N doping. As a typical example, a N-doped 3D graphene foam (3D-NG) was prepared through a chemical vapor deposition (CVD) method, which achieved a CO FE of 85% at a low overpotential of -0.47 V.[28] The high CO selectivity of 85% for 3D-NG at low overpotential was outstanding among those reported Nano-CNMs for ECR so far. The high resolution N 1s XPS spectrum revealed that the content of pyridinic-N was up to 4.1 at.% when pyrolysis at 800 °C and the activity is optimal. Therefore, the high ECR activity was attributed to the formation of active sites induced by pyridinic-N dopants. In addition, it should be noted that the synthesis method can be further extended to fabricate the pyridinic-N doped carbon nanotubes (NCNTs), which manifested a maximum CO selectivity of 80%, slightly lower than that of 3D-NG, and the unprecedented overpotential of -0.18 V for the NCNTs still makes this work more energy efficient and practical for applications.[21] The pyridinic-N in the NCNTs was recognized as real catalytic site to selectively convert CO_2 for CO production, as it is beneficial to the formation of intermediates and desorption of CO molecules (Figure 1b).

Compared with the complex CVD method, other simple synthesis methods have also been employed to prepare the N-doped Nano-CNMs catalysts. For example, N-doped graphene nanoribbon networks (N-GRW) with tunable types and contents of N dopants were successfully synthesized by a high-temperature pyrolysis approach (Figure 1c). The N-GRW electrocatalyst exhibited superior ECR catalytic activity, with a much higher CO FE of 87.6% than the above-mentioned 3D-NG at a mild overpotential of -0.49 V. As shown in Figure 1d, the pyridinic-N was blocked by the phosphate

anion, resulting in a decrease of the catalytic activity. Thus, the activity could be attributed to the activation of pyridine N and the DFT result also supported this claim (Figure 1e).[22] Along this line, the high-temperature pyrolysis method was further utilized to synthesize the N-doped carbon nanotubes (NCNTs) with different contents of pyridinic-N by adjusting the precursors. When the pyridinic-N contents increased from 0.3 at.% to 1.1 at.%, the CO FE of NCNTs was enhanced from 14% to 80%, demonstrating that the pyridinic-N in the NCNTs likely acted as the major active sites for ECR.[29] In addition to graphene and CNTs, other carbon-based precursors (e.g., polymers) were also employed as precursors to synthesize the Nano-CNMs for ECR. For instance, metal-free N-doped carbon nanofibers (CNFs) were obtained by pyrolysis treatment of electrospun polyacrylonitrile (PAN) solution,[31] and the obtained CNFs could convert CO_2 into CO with a CO FE of 98% at a very low overpotential of -0.17 V, which was the lowest among all above-mentioned ECR electrocatalysts. Raman spectroscopy suggested that the N defects were integrated into the carbon lattice. Theoretical calculations and experimental characterizations demonstrated that the high ECR performance was attributed to the interactions between the dopant N atoms and their adjacent C atoms, which redistributed the charge and spin density of prepared CNFs.

In addition to the chemicals, plant biomass materials can also be used as raw precursors to synthesize the Nano-CNMs catalysts. For instance, a N-doped hierarchical honeycomb porous carbon (NDC) was synthesized by a facile one-step pyrolysis treatment of wheat flour. In spite of the NDC only displaying a CO selectivity of 83.7%, the durable NDC electrocatalyst can continuously convert CO_2 to CO for more than two days.[20] Besides, solid fossil fuels can be directly used as carbon sources through doping to prepare Nano-CNMs. As a typical example, the bituminous coal as a precursor was treated with ammonia to prepare the N-doped porous carbon (CNPC).[32] In order to explore the effect of the N configurations, the calcination temperature was adjusted. XPS analysis showed that the relative content of pyridinic-N increased to the maximum at 1100 °C and CO FE reached maximum at the same time. Thus, pyridinic-N was considered to play an important role on ECR. In addition, the commercial activated carbon BAX derived N-doped porous nanocarbons were successfully prepared through a simple carbonization treatment at high temperature under nitrogen (N_2) flowing, and the achieved N-doped porous nanocarbons performed well for the CO formation with 40% FE *via* ECR.[33] Notably, the linear relationship between the content of pyridinic-N and CO FE has been fitted, which proved that the pyridinic-N was crucial for ECR.

2.2. Metal-free other heteroatom (F, S, or B)-doped carbon materials

Similar with the N atoms, the more electronegative F and S atoms and the less electronegative B atom (relative to C atoms) could also modify the electronic structure of the adjacent carbon atoms, achieving an asymmetric distribution of spin density,[34] which resulted in similar electrocatalytic properties between other heteroatom (F, S, or B) doped Nano-CNMs with that of N-doped Nano-CNMs.[34-37] For instance, a F-doped carbon (F-C) electrocatalyst with porous structure was synthesized by a facile pyrolysis process (Figure 2a).[38] Benefitting from the F dopants, the F-C catalyst enabled the maximum CO FE of 90% at a low overpotential of -0.51 V for ECR (Figure 2b). Compared with pristine carbon, F-C possessed abundant defects and large surface area as confirmed by Raman spectroscopy and N_2 adsorption-desorption isotherms. With activation of F atoms, the neighboring carbon atoms tightly adsorbed the *COOH intermediate and favorably acted as an energy barrier for hydrogen evolution reaction (HER), based on DFT calculations (Figure 2c). Similarly, although the active sites of S atoms could stabilize the *COOH intermediates, the S-doped carbon (S-C) materials tended to produce methane with few amount of CO formation (CO FE of ~2%).[39] Likewise, B-doped carbon materials may be disinclined to produce CO. For example, a B-doped graphene (BG) could mainly convert CO_2 to formic acid, and there were a few amounts of CO formation.[40] In view of the unsatisfactory ECR performance of single heteroatom dopants, the multiple heteroatoms co-doped carbon materials were developed to increase the type and activity of heteroatoms dopants. For instance, S, N, co-doped carbon materials synthesized *via* a

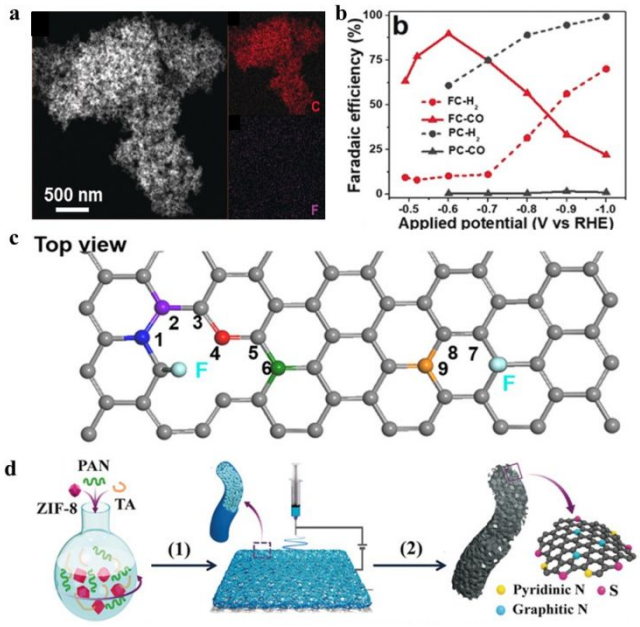

Figure 2. (a) High-angle annular dark field-scanning transmission electron microscopy (HAADF-STEM) image and corresponding elemental mappings of F-C. (b) FEs of CO and H_2 productions. (c) Top view of DFT model for F-C. Gray atom: carbon, light blue atom: F, other colorful atoms: carbon that calculated as active sites. Reproduced with permission from ref. 38, Copyright 2018, Wiley-VCH. (d) A schematic illustration of synthesis process for NSHCF. Reproduced with permission from ref. 41, Copyright 2018, Wiley-VCH.

REVIEW

Table 1. Summary of other reported metal-free heteroatoms-doped carbon materials for CO production *via* ECR.

Catalyst	Synthesis method	Electrolyte	Loading amount [mg cm^{-2}]	Max FE [%]	Potential Vs RHE @MaxFE	Jco @MaxFE [mA cm^{-2}]	Cell type
NDC[20]	Pyrolysis	0.5 M $NaHCO_3$	2.8	83.7	-0.82	6.6	H-cell
NCNTs[21]	CVD	0.1 M $KHCO_3$	0.5	80	-0.8	~0.75	GDE
3D-NG[28]	CVD	0.1 M $KHCO_3$	0.3-0.5	85	-0.58	~1.8	GDE
Microporous NCNTs[29]	Pyrolysis	0.1 M $KHCO_3$	0.5	80	-1.05	~3.5	GDE
CN-H-CNTs[30]	Hydrothermal steam etching	0.1 M $KHCO_3$	--	88	-0.5	~10	H-cell
N-GRW[22]	Pyrolysis	0.5 M $KHCO_3$	0.2	87.6	-0.4	~5	H-cell
CNFs[31]	Pyrolysis	EMIM-BF_4	~2.5	98	-0.973	~3.5	Single-cell
CNPS[32]	Pyrolysis	0.1 M $KHCO_3$	0.2	92	-0.6	~0.9	H-cell
N-doped BAX-M-950[33]	Pyrolysis	0.1 M $KHCO_3$	--	40	-0.75	--	H-cell
F-C[38]	Pyrolysis	0.1 M $NaClO_4$	0.2	90	-0.62	~0.26	H-cell
S-C[39]	Pyrolysis	0.1 M $KHCO_3$	2.5	--	--	--	H-cell
BG[40]	Pyrolysis	0.1 M $KHCO_3$	--	--	--	--	H-cell
S, N-C[39]	Pyrolysis	0.1 M $KHCO_3$	2.5	11.3	-0.99	~0.1	H-cell
NSHCF[41]	Pyrolysis	0.1 M $KHCO_3$	1.2	94	-0.7	~103	H-cell
N,S-codoped carbon layers[42]	Pyrolysis	0.1 M $KHCO_3$	0.8	92	-0.6	2.63	H-cell
ZIF-8 mediated NC[43]	Pyrolysis	0.1 M $KHCO_3$	~4	78	-0.93	1.1	H-cell
NCNT[44]	Pyrolysis	0.1 M $KHCO_3$	6.6	90	-0.9	~0.8	H-cell

pyrolysis treatment of electrospinning polymer nanofibers (Figure 2d) were reported to exhibit a much higher ECR catalytic activity than the S-doped carbon materials.[41] The CO selectivity of S, N, co-doped hierarchically porous carbon nanofiber (NSHCF) was significantly improved to be 94% with more than 100 mA cm^{-2} current density, but it was a little bit lower than that of N-doped CNFs. It was believed that the pyridinic-N was more active than thiophene S for the ECR, and the N doping was more likely to be capable of stabilizing the *COOH intermediates. On the other hand, previous reports demonstrated that S dopant could also act as a coadjutant to increase the content of pyridinic-N and suppress the formation of graphitic-N.[42] X-ray photoelectron spectroscopy (XPS) results showed that after doping of S into N-doped carbon, the content of pyridinic-N increased from 43% to 52%, and graphitic-N decreased from 52% to 44%, thus resulting in the maximum CO FE increased from 75% to 92%. Such an increase in CO FE could be attributed to the fact that the S dopant provided more edge positions to host high-density pyridinic-N.

3. Transition metal heteroatoms complex doped carbon materials

Although the doping of heteroatoms could improve ECR catalytic performance of nanocarbon materials, the electrocatalytic activity and efficiency of these metal-free heteroatoms-doped carbon materials are still far from satisfactory due to scant active sites.[45]

Further introduction of transition metals into heteroatoms-doped nanocarbons could greatly enhance ECR catalytic activity, because their partially filled d-orbital electrons that are very close to Fermi level could chemically optimize the electronic structures and overcome the intrinsic activation barriers of heteroatoms-doped nanocarbons. This enhances the reaction kinetics, subsequently promoting the formation of intermediates.[46, 47] In addition, low cost, high selectivity, and high energy efficiency make transition metal heteroatoms complex doped carbon materials as a promising candidate for ECR electrocatalysts.[48]

3.1. Transition metal-N complex doped carbon materials

Transition metal-N complex doped carbon materials (M-N-C) have recently been reported and acted as a kind of N-doped Nano-CNMs with unique structure of active sites, such as Ni-N-C, Fe-N-C, Co-N-C, and Mn-N-C, *etc*.[49-51] In those M-N-C materials, the N atoms are coordinated with transition metal center forming catalytically active sites. The active sites are similar to those reported molecules structure of phthalocyanine, which have been proposed with ECR catalytic activity. The M-N-C materials are considered as promising alternative electrocatalysts for ECR not only due to the outstanding catalytic performance, but also they can be prepared by using cheap precursors *via* simple synthesis method.[52] For the ECR, DFT calculations revealed that the M-N-C materials possess much lower absorption free energy for *COOH intermediates than transition metal nanoparticles (NPs) directly loaded on the surface of nanocarbons.[53] In addition, the interactions of transition metal with N atoms could increase the speed of charge transfer and greatly reduce the local work function of nanocarbons to prompt the ECR reaction.[54] In light of the unique structural characteristics, different synthesis methods were widely developed to prepare the M-N-C materials (Figure 3a). For example, a Ni and N modified graphene (Ni-N-Gr) was synthesized by annealing the metal complex and graphene oxide (GO) composite at high temperature. The Ni and N elements were observed to disperse uniformly on the graphene by energy-dispersive X-ray (EDX) analysis, while no Ni species were observed in X-ray diffraction (XRD) pattern. The Ni-N-Gr exhibited a CO FE of > 90% at the potentials from -0.7 to -0.9 V.[55] Such a high ECR selectivity could be attributed to the unique formation of Ni-N-C structure, which could be well retained without obvious NPs aggregation using an appropriate heat treatment process. Notably, this was the first report on Ni-N-C catalyst with excellent ECR performance. To obtain the more isolated Ni-N_x-C catalyst with excellent ECR performance, a nanocarbon ECR catalyst with high loading amount of Ni single atom (5.44 wt.%) was prepared by a pyrolysis treatment of zeolitic imidazolate frameworks (ZIF) containing Ni ions, denoted as C-Zn_xNi_y ZIF-8 (Figure 3c). After pyrolysis, all elements were uniformly distributed in the C-Zn_xNi_y ZIF-8 (Figure 3b).[56] By regulating the Ni contents, the C-Zn_1Ni_4 ZIF-8 achieved a CO FE of over 92% under a wide potential window between -0.53 to -1.03 V vs RHE, much higher than the aforementioned Ni-N-Gr material's FE for CO production, which was only 90%. The high ECR catalytic activities might be due to the fact that the most Ni-N_4-C structure was retained to a greater extent avoiding the conversion of the Ni atoms into Ni NPs. Along this line, other Ni-N-C materials were constructed. As shown in Figure 3d, Ni species highlighted by red circles were atomically dispersed into the graphene, not nanoclusters or particles. It displayed a maximum CO FE of 99% with current density of 28.6 mA cm^{-2}.[57] Such an ECR activity of Ni-N-C could significantly suppress the competitive HER because the presence of Ni-N-C structure efficiently inhibited the formation of HER intermediates. Theoretical calculations revealed that after absorbing CO_2 molecules, the free energy of the *COOH intermediates formed by Ni-N_4 sites was lower than that of NC structure. Ni-N_4 significantly reduced the rate determining step of

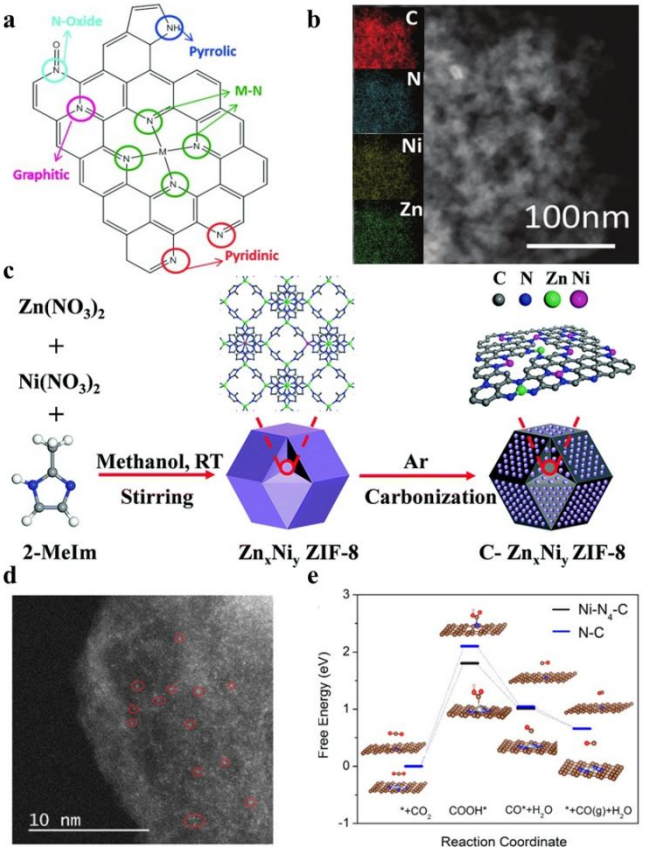

Figure 3. (a) Structural models of M-N-C. Reproduced with permission from ref. 55, Copyright 2015, Wiley-VCH. (b) HAADF-STEM image of C-Zn_1Ni_4 ZIF-8 and corresponding energy-dispersive X-ray spectroscopy (EDS) images for C, N, Ni, and Zn in C-Zn_1Ni_4 ZIF-8. (c) Schematic illustration of the synthesis process for C-Zn_xNi_y ZIF-8. Reproduced with permission from ref. 56, Copyright 2018, The Royal Society of Chemistry. (d) HAADF-STEM image of Ni-N_4. (e) Calculated free energy diagram. Reproduced with permission from ref. 57, Copyright 2017, American Chemical Society.

the reaction barrier, which contributed to the high ECR activity for CO production (Figure 3e). However, for industrial applications, conversion rates are more important than selectivity. Thus, Ni-N-C gas diffusion electrode (GDE) and flow cell were constructed to realize practical applications. Notable, when the current density was up to 200 mA cm^{-2}, the CO yield was significantly better than that of noble Ag catalyst.[58] Besides the Ni-N-C materials, other transition metals-N complex doped carbon based catalysts, such as Fe-N, Co-N, and Mn-N *etc.*, with excellent ECR performances have also been prepared.[59-62] For instance, an isolated Fe^{3+}-N-C was prepared *via* a pyrolysis treatment of iron containing ZIF-8, and the oxidation state of Fe^{3+} species was well maintained in this system to improve CO_2 adsorption. When operating in a flow-cell, the CO partial current density reached industrial application level of nearly 100 mA cm^{-2} at ultra-low overpotential of around 340 mV.[59] The effect of valence state of metal center on ECR activity was discussed in depth. The higher valence (+3) of metal center was not only beneficial to CO_2 adsorption, but also weakened the CO binding at metal center, which indicated that the reaction was not limited by CO desorption step. As a result, the higher current density of Fe^{3+}-N-C via ECR could be achieved as compared with that of Fe^{2+}-N-C. Due to the variable valences of Mn element, there are few studies on the Mn-based nanocarbon materials as efficient electrocatalysts for ECR, but the electrocatalytic activity of Mn species could still be enhanced by optimizing its electronic structure. As a typical example, a chlorine (Cl) and N dual-coordination Mn dispersed on graphene (Cl,N-Mn/G) catalyst was prepared by a one-step pyrolysis method using as performed Mn-ethylenediamine-Cl polymer. The structure of Cl atom axial suspension on Mn-N_4 was confirmed by Mn K-edge X-ray absorption near-edge structure (XANES) and extended X-ray absorption fine structure (EXAFS). Compared with only N corrdination Mn dispersed graphene (N-Mn/G), the Cl,N-Mn/G showed the superior high turnover frequency (TOF) of 38347 h^{-1} and outstanding selectivity, which was attributed to the fact that unique electronic structure of Mn species significantly reduced the formation barriers of *COOH intermediates.[61]

3.2. Transition metal-other heteroatom complex doped carbon materials

Despite certain researches, the applications of M-N-C in ECR are still in infancy, to improve the overall catalytic activity, other different types of Nano-CNMs catalysts comprised with transition metals and heteroatoms (N, P, or S, *etc.*) co-doped nanocarbons were also constructed. Theoretical studies have showed that due to the strong electronegativity of N adjacent atoms, transition metal atoms have higher reaction free energy for adsorption of intermediate products, which increases the potential barrier in the reaction process. Thus, by introducing suitable foreign atoms, the electron donor properties of transition metal can be adjusted to reduce potential barriers and further improve the intrinsic catalytic activity of M-N-C materials.[63] For instance, a N, P, Co-doped 3D mesoporous carbon frameworks (3D N, P, Co-MPC) was prepared by a self-growth-templating method, achieving a CO FE of 63% for ECR.[64] Besides, a N and S co-doped Fe-containing highly porous carbon (Fe-NS-C) was obtained through a pyrolysis treatment of 2-pyrrolecarboxaldehyde and 2-thiophenecarboxaldehyde organic gel. The achieved Fe-NS-C carbon gel exhibited a CO FE of nearly 85%, which was comparable to the controlled Fe-N-C material.[65] It could be found that besides the N dopants, the introduction of additional S atoms into the Nano-CNMs could not only facilitate the formation of *COOH intermediates, but also increase the porosity and specific surface area of Nano-CNMs, thus improving the ECR activity and selectivity.

4. Carbon-based hybrid materials

Compared with heteroatoms-doped carbon materials and transition metal-heteroatoms complex doped carbon materials, carbon-based

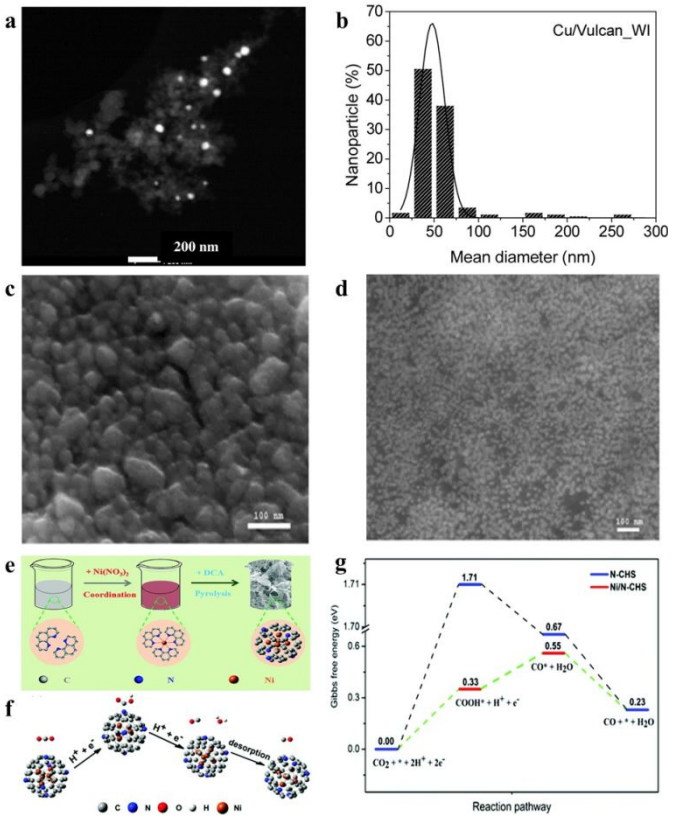

Figure 4. (a-b) Scanning transmission electron microscope (STEM) images and pore size distribution of Cu NPs-CB. Reproduced with permission from ref. 66, Copyright 2017, Elsevier Ltd. (c-d) Scanning electron microscope (SEM) images of Cu NPs and Cu-rGO. Reproduced with permission from ref. 67, Copyright 2017， Nature Publishing Group. (e) Schematic illustration of the synthetic process for the Ni/NCHS. (f) Reaction paths of Ni/NCHS for ECR and (g) Gibbs free energy diagrams on Ni/NCHS. Reproduced with permission from ref. 68, Copyright 2019, The Royal Society of Chemistry.

hybrid materials, as popular Nano-CNMs, could allow for combining the advantages of each material, such as large surface area, high electrical conductivity, and based active sites.[69] Owing to those unique advantages, carbon-based hybrid materials have been recently utilized as a class of effective ECR electrocatalysts for CO production. In the hybrid system, several different kinds of electrocatalysts containing transition metals, transition metal compounds, and metal-free nanocarbon materials were introduced into the nanocarbon based supports, acting as the mediums of charge transport and active centers to enhance the ECR performance.

4.1. Transition metals/carbon-based hybrid materials

Transition metals/carbon-based hybrid materials have been considered as efficient Nano-CNMs catalysts for ECR because they combine the advantages of transition metals as active sites to reduce the energy barriers with the advantages of nanocarbon materials as supports to provide high electron transfer rate and large surface area for the deposition of active materials.[70] For instance, transition metals (Cu, Ni, Fe, and Co, *etc.*) NPs were uniformly deposited on the surface of carbon black (M-CB) by an incipient-wetness impregnation of transition metals ions into CB (Figure 4a-4b).[66] All of these transition metals NPs loaded on the M-CB showed certain ECR catalytic activity, however the overall ECR performances of transition metals NPs-CB for CO production was still not as competitive as the HER performances (CO FE < 10%). This result was mainly because transition metal NPs suffer from difficult control of the loading amounts, thus leading to the excessive NPs serving as the active sites for HER. Following this route, the loading methods of transition metal NPs were further improved for controlled synthesis of transition metals/carbon-based hybrid materials. For instance, a unique carbon-based nanocomposite consisting of Cu NPs and reduced GO (rGO) supported on Cu substrate (Cu-rGO) was prepared by using a facile electrochemical reduction method *via* cyclic voltammetry. Compared with Cu particles, the NPs size after compound with rGO is more uniform (Figure 4c-4d).[67] The higher CO FE of Cu-rGO nanocomposite reached to 40% as compared with that of above-mentioned M-CB. The enhanced ECR catalytic activity could be attributed to the synergistic coupling effects between the Cu NPs and rGO, which makes the CO_2 molecular easier to be absorbed. Considering that the doped carbon materials could facilitate the ECR reaction better than nanocarbon materials, transition metals NPs/doped carbon materials were further designed. For instance, *in situ* encapsulation of Ni NPs into N-doped carbon nanosheets and nanotubes hybrid substrates (Ni/N-CHSs) was achieved by a pyrolysis treatment of the metal ion-benzene complex and dicyandiamide (DCDA) as nitrogen precursor (Figure 4e).[68] TEM and EDX revealed that the Ni NPs were completely encapsulated by carbon layers instead of sticking to the surface. The Ni/N-CHSs showed a CO FE of 93.1% for ECR, which was much higher than the controlled N-doped carbon sample. DFT calculations demonstrated that the Ni NPs assisted N-doped carbon could efficiently tune the electron distribution, thus resulting in the reduction of the reaction barrier for *COOH formation (Figure 4f-4g). Moreover, the positive role of carbon layer coating the NPs has been gradually noticed. For example, the carbon layer coated Ni NPs supported on N-doped carbon (Ni-NC@C) was synthesized by pyrolysis of nickel metal organic frameworks (MOFs) on carbon in argon., and a CO FE of 94% at an overpotential of -0.59 V was achieved. Structural characterizations showed that most of the crystalline Ni NPs were well wrapped by carbon shells, which resulted in the suppressed HER performance compared with that of bare Ni NPs.[71]

4.2. Transition metals compounds/carbon-based hybrid materials

In addition to the transition metals/carbon-based catalysts, transition metal compounds/carbon-based materials with high valences of transition metal ions could also deliver great promise for the ECR, by providing chemical functionality that stabilizes the

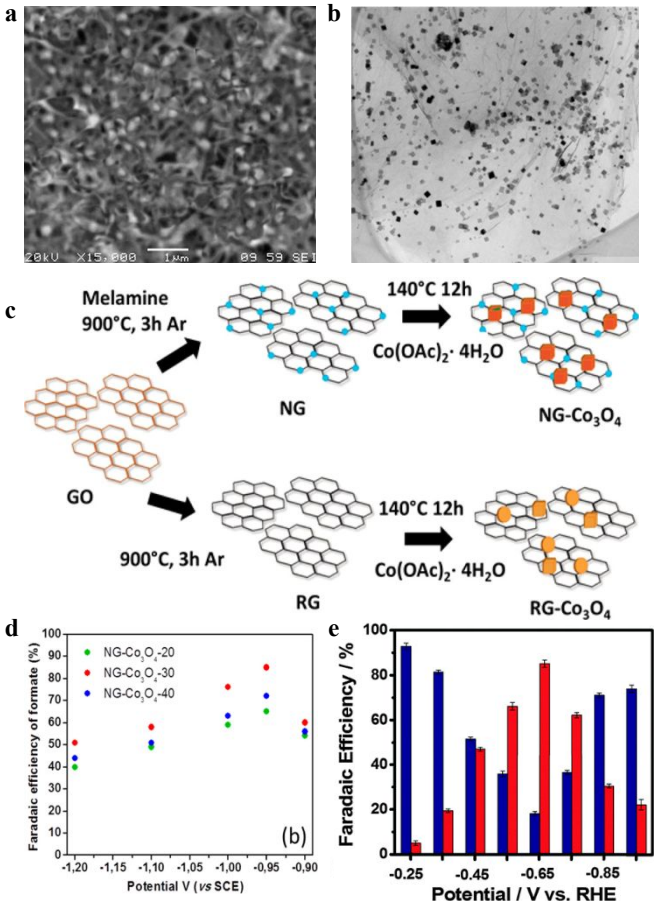

Figure 5. (a) SEM image of NiO/MWCNT. Reproduced with permission from ref. 72, Copyright 2015, Springer Science + Business Media New York. (b) Transmission electron microscope (TEM) image of NG-Co_3O_4. (c) Synthesis method of NG-Co_3O_4. (d) CO FE of NG-Co_3O_4. Reproduced with permission from ref. 73, Copyright 2017, American Chemical Society. (e) FEs of CO (red bars) and H_2 (blue bars) for rGO-PEI-MoS_x. Reproduced with permission from ref. 74, Copyright 2016, The Royal Society of Chemistry.

REVIEW

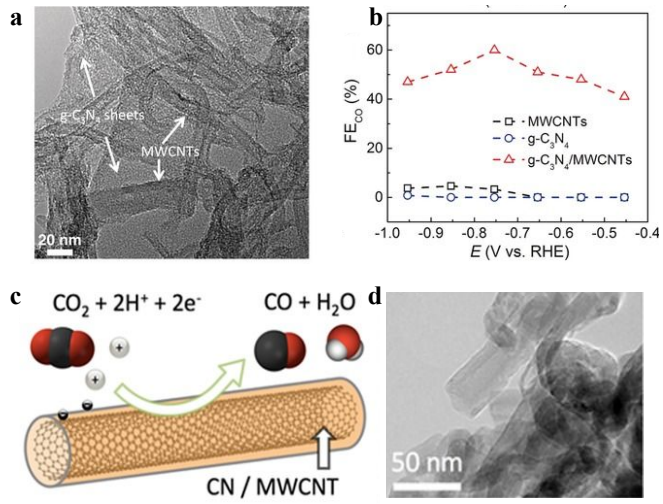

Figure 6. (a) TEM image of g-C_3N_4/MWCNT. (b) FEs of CO for g-C_3N_4/MWCNT. Reproduced with permission from ref 75, Copyright 2016, Wiley-VCH. (c) Representation of the ECR on CN/MWCNT. (d) TEM image of CN/MWCNT. Reproduced with permission from ref 76, Copyright 2017, Wiley-VCH.

incipient negative charge on CO_2 molecules or by mediating the electron transfer directly.[77] Among various transition metal compounds, transition metal oxides are the most common and widespread form in nature. However, on account of the low number of active sites and poor CO selectivity, transition metal oxides are not ideal ECR electrocatalysts for CO production.[78] Up to now, only a few carbon-based transition metal oxides hybrids have been reported as efficient Nano-CNMs for ECR. As a typical example, the NiO impregnated onto multi-walled carbon nanotube (MWCNT) to form the NiO/MWCNT composite was achieved by a pyrolysis treatment of MWCNT impregnated with Ni salt (Figure 5a).[72] The CO FE of NiO/MWCNT composite was only about 5%, which was much lower than that of other heterogeneous carbon-based materials. Following this step, a hybrid ECR catalyst formed with loading Co_3O_4 on the surface of NG (NG-Co_3O_4) was prepared by a hydrothermal treatment of Co iron adsorbed NG (Figure 5b-5c).[73] Although the CO FE of 10-20% for NG-Co_3O_4 was far higher than that of NiO/MWCNT, and even comparable to that of the above-mentioned transition metal NPs-CB, the CO selectivity of NG-Co_3O_4 catalyst still remained unsatisfactory for practical applications (Figure 5d). Apart from the transition metal oxides, nanocarbon-based transition metal sulfides have also been reported as efficient ECR electrocatalysts due to their prominent catalytic features and high conductivities. A representative work was to load molybdenum sulphide (MoS_x) onto the surface of polyethylenimine (PEI)-modified rGO to form rGO-PEI-MoS_x hybrid (Figure 5e).[74] Compared with NG-Co_3O_4 and NiO/MWCNT materials, the rGO-PEI-MoS_x hybrid showed outstanding ECR activity and CO selectivity with a high CO FE of 85.1%, mainly attributed to the unique structure of MoS_x, in which each Mo atom was coordinated to six S ligands. The unique structure was similar with the formate dehydrogenases (FDH) enzyme that can catalyze the reduction of CO_2. Besides, the introduced PEI layer could further enhance the ECR activity of Mo-S sites and stabilize the *COOH intermediate.

4.3 Metal-free/carbon-based hybrid materials

Although both transition metals/carbon and transition metal compounds/carbon catalysts exhibited high ECR catalytic performances, the high cost, sensitivity to poisoning, and difficulty of reclamation largely limited their practical applications for CO_2-CO conversion, which motivate researchers to pay more attention to the metal-free/carbon-based hybrid ECR materials. Among metal-free/carbon-based hybrid catalysts, g-C_3N_4 is an important metal-free material which has received more and more attention in the fields of photocatalysis and electrocatalysis. Despite its low electrical conductivity, the g-C_3N_4 can reveal its electrochemical properties by complexing with other nanocarbons, originating unique chemical and electronic coupling effects between them. DFT calculations revealed that the g-C_3N_4 as a molecular scaffold could appropriately modify the electronic structure of the loading materials, lowering the free energy of intermediates, and consequently easing their stabilization. Also, the adsorption capacity of CO_2 molecules can be improved because of the stronger electronegativity of N atoms compared with C atoms. As for ECR, it DCDA precursors (Figure 6a).[75] The sp^3 C-N peak was absent in the XPS C 1s spectra of g-C_3N_4/MWCNT, which indicated that the g-C_3N_4 was recently reported that a g-C_3N_4 and MWCNT composite was formed by a polycondensation process between the MWCNTs and was covalently attached onto MWCNTs. The obtained g-C_3N_4/MWCNT hybrid achieved the high ECR catalytic activity with CO FE of 60% (Figure 6b) and over 50 h of significant durability, in which the g-C_3N_4 provided more active sites and the covalent C-N bonding in the MWCNT enhanced the ECR activities. Similar to this work, a N-doped carbon (CN)-coated MWCNT (CN-MWCNT) nanocomposite was prepared *via* a pyrolysis treatment of the g-C_3N_4 and MWCNT mixture (Figure 6c-6d), and the excellent ECR catalytic properties was obtained with approximately 98% FE for CO production.[76]

Table 2. Summary of other reported transition metal-heteroatoms complex doped carbon materials and carbon-based hybrid materials for CO production via ECR.

Catalyst	Synthesis method	Electrolyte	Loading amount [mg cm^{-2}]	Max FE [%]	Potential Vs RHE @MaxFE	Jco @MaxFE [mA cm^{-2}]	Cell type
A-Ni-NG[54]	Pyrolysis	0.5 M $KHCO_3$	0.1	97	-0.5	22	H-cell

Catalyst	Synthesis method	Electrolyte	Loading amount [mg cm^{-2}]	Max FE [%]	Potential Vs RHE @MaxFE	Jco @MaxFE [mA cm^{-2}]	Cell type
Ni-N-Gr[55]	Pyrolysis	0.1 M $KHCO_3$	0.3	90	-0.7	--	H-cell
Ni-N_4-C[56]	Pyrolysis	0.1 M $KHCO_3$	2	98	-1.03	71.5	H-cell
Ni-N-C[57]	Pyrolysis	0.1 M $KHCO_3$	6.4	99	-0.81	28.6	H-cell
Ni-N-C[58]	Pyrolysis	0.1 M $KHCO_3$	1	90	-1.0	~180	GDE
Fe^{3+}-N-C[59]	Pyrolysis	0.5 M $KHCO_3$	0.3	~95	-0.5	~100	GDE
(Cl, N)-Mn/G[61]	Pyrolysis	0.5 M $KHCO_3$	0.5	95	-0.6	~10	H-cell
Co-N_5/HNPCSs[60]	Pyrolysis	0.2 M $NaHCO_3$	0.4	99.4	-0.79	~4.5	H-cell
Ni-NG[79]	Pyrolysis	0.1 M $KHCO_3$	0.2	97	-0.66	~50	GDE
Ni-NCB[80]	Pyrolysis	0.5 M $KHCO_3$	0.2	99	-0.681	~100	GDE
NiSA-N-CNTs[81]	Pyrolysis	0.5 M $KHCO_3$	1	91.3	-0.7	~23	H-cell
Fe-N_4/CF[82]	Pyrolysis	0.5 M $KHCO_3$	2	94.9	-0.5	~3	H-cell
Fe-ZIF-8 derived Fe-N-C[83]	Pyrolysis	0.5 M $KHCO_3$	0.459	93.5	-0.5	~15	H-cell
Fe-N-C[84]	Pyrolysis	0.5 M $NaHCO_3$	--	90	-0.5	6	H-cell
Fe/NG[85]	Pyrolysis	0.1 M $NaHCO_3$	0.32	80	-0.6	~1.5	H-cell
Zn-N_x/C[86]	Pyrolysis	0.5 M $KHCO_3$	~0.4	95	-0.43	4.8	H-cell
Zn-N-G[87]	Pyrolysis	0.5 M $KHCO_3$	2	90.8	-0.5	~3	H-cell
3D N, P, Co-MPC[64]	Pyrolysis	0.1 M $KHCO_3$	2	62	-0.3	--	H-cell
Fe-NS-C[65]	Pyrolysis	0.1 M $KHCO_3$	0.3	85	-0.62	--	H-cell
Cu-rGO[67]	Electroreduction	0.1 M $NaHCO_3$	--	40	-0.6	--	Single-cell
Ni/N-CHSs[68]	Pyrolysis	0.5 M $KHCO_3$	0.5	93.1	-0.9	~15	H-cell
Ni-NC@C[71]	Pyrolysis	0.5 M $KHCO_3$	0.1	93.7	-0.7	~7	H-cell
Ni@NCNTs[88]	Pyrolysis	0.5 M $KHCO_3$	1	99.1	-0.9	~10	H-cell
rGO-PEI-MoS_x[74]	Electrodeposition	0.5 M $NaHCO_3$	--	85.1	-0.65	--	H-cell
g-C_3N_4/MWCNTs[75]	Polycondensing	0.1 M $KHCO_3$	0.36	60	-0.75	~0.6	H-cell
CN-MWCNT[76]	Pyrolysis	0.1 M $KHCO_3$	2.39	98	-0.82	~70	GDE

REVIEW

5 Conclusion and Outlook

In summary, this review reports an overview of the recent developments regarding Nano-CNMs ECR catalysts for electrocatalytic conversion CO_2 into CO production. Emerging Nano-CNMs are represented by metal-free heteroatoms-doped carbon materials, transition metal-heteroatoms complex doped carbon materials and carbon-based hybrid materials; great progresses have been made for Nano-CNMs in improving ECR selectivity, activity, and stability. For metal-free heteroatoms (e.g., N, F, S, and B) doped carbon materials, the advantages of superior durability and low cost enable them to be competitive candidates to replace the noble metal catalysts for the ECR. Typically, the introduction of N atoms shows certain capability to regulate the distribution of charge density and increase the electron transfer rate of nanocarbons, thus boosting the overall ECR performances. For further enhancing ECR performance, the types and contents of heteroatoms dopants need to be finely tuned by using the different synthesis methods, such as stream etching, CVD, and pyrolysis approaches. For transition metal-heteroatoms complex doped carbon materials, further introduction of transition metal atoms could address the problems of low ECR catalytic activity of metal-free heteroatoms-doped carbon materials. The partially filled d orbital electrons of transition metals can overcome the inherent activation barriers, while enhance reaction kinetics to improve the ECR activity. Furthermore, the carbon-based hybrid materials possess better flexibility because it can combine the advantages of different catalysts with their variable assembly possibilities, when compared with the two types of above-mentioned catalysts.

Although extensive studies have been conducted in the development of Nano-CNMs ECR catalysts achieving considerable progress, the research for selective electrocatalysis for CO production via ECR is still in its developing stage, and more fundamental and insightful studies with a goal to address the pressing issues and daunting challenges faced in this fields, are needed.

(I) During the research process of ECR electrocatalysts, the standardization of data collection was a problem worthy of attention. Especially for Nano-CNMs, several factors could affect the performance evaluation of electrocatalysts, such as, selection of test benchmark, the influence of the hydrodynamics of the electrochemical cell, and effect of impurities in electrolyte.[89] Among those factors, the impurities are easier to be ignored while potentially impacted the quality of data collection. Due to the outstanding stability, Pt was chosen as counter electrode in most three-electrode cell configuration. However, Pt was inevitably dissolved in the electrolyte and then deposited on the cathode during electrochemical cycling, thus resulting in the inaccurate evaluation of intrinsic activity of electrocatalysts. Therefore, several suitable substitutes have been proposed to avoid the effects of Pt impurity, for example, the glassy carbon was used as counter electrode.[90] However, since Pt was used as the counter electrode in the initial ECR study, this measurement method has even been deployed for performance evaluation with precious metal-free materials, and only a few researchers realized this question and tried to replace the Pt electrode. Therefore, if Pt was used as counter electrode, controlled experiments are necessary to prove no altered ECR performance at least.

(II) In spite of certain breakthroughs that have been made in ECR selectivity, activity, and stability, how to balance the above three indicators is still a question. The types and contents of heteroatoms dopants, the structures of active sites, and the morphologies of catalysts have significant effect on the ECR performances of Nano-CNMs. Consequently, advanced synthetic methods need to be developed to realize controllable synthesis of Nano-CNMs.

(III) Unlike the explicit HER mechanism, CO production via ECR involving competitive reactions that makes the studies of ECR mechanism more difficult in modeling and theoretical calculations. Although a few assumptions about catalysts and specific reaction processes have been proposed, a comprehensive and in-depth understanding of the ECR catalytic mechanism is still missing. Further theoretical calculation models and methods accompanied with experimental explorations could help us to better understand the reaction process, and gradually break through the bottlenecks of the reaction control step, thus comprehensively improving the ECR performance.

(IV) In order to accurately analyze the origin of active sites and clarify the reaction mechanisms, advanced analysis methods that can reveal the changes of ECR catalysts during the reaction process and trace the reactants at the molecular level are necessary, such as operando techniques using X-ray powder diffraction, X-ray photoelectron spectroscopy, Raman spectroscopy, and X-ray absorption spectroscopy, *etc.*

Acknowledgements

This work was financially supported by National Natural Science Foundation of China (21922811, 51702284, 21878270), Zhejiang Provincial Natural Science Foundation of China (LR19B060002), and the Startup Foundation for Hundred-Talent Program of Zhejiang University (Y. Hou). G. Wu acknowledges the support from National Science Foundation (CBET-1804326).

Notes and References

1. H. Rao, L. C. Schmidt, J. Bonin and M. Robert, *Nature*, 2017, 548, 74-77.
2. M. Asadi, K. Kim, C. Liu, A. V. Addepalli, P. Abbasi, P. Yasaei, P. Phillips, A. Behranginia, J. M. Cerrato, R. Haasch, P. Zapol, B. Kumar, R. F. Klie, J. Abiade, L. A. Curtiss and A. Salehi-Khojin, *Science*, 2016, 353, 467-470.
3. A. K. Singh, J. H. Montoya, J. M. Gregoire and K. A. Persson, *Nat. Commun.*, 2019, 10, 443.
4. J. Gallagher, *Nat. Energy*, 2016, 1, 15024.
5. K. Xu, B. Sun, J. Lin, W. Wen, Y. Pei, S. Yan, M. Qiao, X. Zhang and B. Zong, *Nat. Commun.*, 2014, 5, 5783.
6. W. Ju, A. S. Varela, P. Strasser, A. Bagger, J. Rossmeisl, G.-P. Hao, V. Bon, S. Kaskel, A. S. Varela, I. Sinev, C. B. Roldan and C. B. Roldan, *Nat. Commun.*, 2017, 8, 944.
7. I. Azcarate, C. Costentin, M. Robert and J.-M. Savéant, *J. Am. Chem. Soc.*, 2016, 138, 16639-16644.

8. S. Back, J. Lim, N. Y. Kim, Y. H. Kim and Y. Jung, *Chem. Sci.*, 2017, 8, 1090-1096.
9. M. Bersani, K. Gupta, A. K. Mishra, R. Lanza, S. F. R. Taylor, H.-U. Islam, N. Hollingsworth, C. Hardacre, N. H. de Leeuw and J. A. Darr, *ACS Catal.*, 2016, 6, 5823-5833.
10. Z. Lei, Z. Zhi-Jian and G. Jinlong, *Angew. Chem. Int. Ed.*, 2017, 56, 11326-11353.
11. S. Zhao, Z. Tang, S. Guo, M. Han, C. Zhu, Y. Zhou, L. Bai, J. Gao, H. Huang, Y. Li, Y. Liu and Z. Kang, *ACS Catal.*, 2018, 8, 188-197.
12. Y. Fang and J. C. Flake, *J. Am. Chem. Soc.*, 2017, 139, 3399-3405.
13. M. Dunwell, Q. Lu, J. M. Heyes, J. Rosen, J. G. Chen, Y. Yan, F. Jiao and B. Xu, *J. Am. Chem. Soc.*, 2017, 139, 3774-3783.
14. S. Back, M. S. Yeom and Y. Jung, *ACS Catal.*, 2015, 5, 5089-5096.
15. M. Cho, J.-W. Seo, J. T. Song, J.-Y. Lee and J. Oh, *ACS Omega*, 2017, 2, 3441-3446.
16. E. L. Clark, C. Hahn, T. F. Jaramillo and A. T. Bell, *J. Am. Chem. Soc.*, 2017, 139,15848-15857.
17. Y. Wu, J. Jiang, Z. Weng, M. Wang, D. L. J. Broere, Y. Zhong, G. W. Brudvig, Z. Feng and H. Wang, *ACS Cent. Sci.*, 2017, 3, 847-852.
18. N. Elgrishi, M. B. Chambers, X. Wang and M. Fontecave, *Chem. Soc. Rev.*, 2017, 46, 761-796.
19. Y. He, X. Zhuang, C. Lei, L. Lei, Y. Hou, Y. Mai and X. Feng, *Nano Today*, 2019, 24, 103-119.
20. F. Li, M. Xue, G. P. Knowles, L. Chen, D. R. MacFarlane and J. Zhang, *Electrochim. Acta*, 2017, 245, 561-568.
21. W. Jingjie, Y. Ram Manohar, L. Mingjie, P. S. Pranav, T. Chandra Sekhar, M. Lulu, Z. Xiaolong, Z. Xiao-Dong, I. Y. Boris, L. Jun and M. A. Pulickel, *ACS Nano*, 2015, 9,5364-5371.
22. S. Liu, H. Yang, X. Huang, L. Liu, W. Cai, J. Gao, X. Li, T. Zhang, Y. Huang and B. Liu, *Adv. Funct. Mater.*, 2018, 28, 1800499.
23. T. Ma, Q. Fan, H. Tao, Z. Han, M. Jia, Y. Gao, W. Ma and Z. Sun, *Nanotechnology*, 2017, 28, 472001.
24. X. Duan, J. Xu, Z. Wei, J. Ma, S. Guo, S. Wang, H. Liu and S. Dou, *Adv. Mater.*, 2017, 29, 1701784.
25. T. Ma, Q. Fan, X. Li, J. Qiu, T. Wu and Z. Sun, *J. CO_2 Util.*, 2019, 30, 168-182.
26. A. Vasileff, Y. Zheng and S. Z. Qiao, *Adv. Energy Mater.*, 2017, 7, 1700759.
27. L. Qiao, W. Zheng, H. Xu, L. Zhang and Q. Jiang, *J. Chem. Phys., 126,* 2007, 164702.
28. J. Wu, M. Liu, P. P. Sharma, R. M. Yadav, L. Ma, Y. Yang, X. Zou, X. D. Zhou, R. Vajtai, B. I. Yakobson, J. Lou and P. M. Ajayan, *Nano Lett.*, 2016, 16, 466-470.
29. P. P. Sharma, J. Wu, R. M. Yadav, M. Liu, C. J. Wright, C. S. Tiwary, B. I. Yakobson, J. Lou, P. M. Ajayan and X. D. Zhou, *Angew. Chem. Int. Ed.*, 2015, 54, 13701-13705.
30. X. Q. Cui, Z. Y. Pan, L. J. Zhang, H. S. Peng and G. F. Zheng, *Adv. Energy Mater.*, 2017, 7, 1701456.
31. B. Kumar, M. Asadi, D. Pisasale, S. Sinha-Ray, B. A. Rosen, R. Haasch, J. Abiade, A. L. Yarin and A. Salehi-Khojin, *Nat. Commun.*, 2013, 4, 2819.
32. C. Li, Y. Wang, N. Xiao, H. Li, Y. Ji, Z. Guo, C. Liu and J. Qiu, *Carbon*, 2019, 151, 46-52.
33. W. Li, B. Herkt, M. Seredych and T. J. Bandosz, *Appl. Catal. B-Environ.*, 2017, 207, 195-206.
34. J. Duan, S. Chen, M. Jaroniec and S. Z. Qiao, *ACS Catal.*, 2015, 5, 5207-5234.
35. W. Cermignani, T. E. Paulson, C. Onneby and C. G. Pantano, *Carbon*, 1995, 33, 367-374.
36. T. J. Li, M. H. Yeh, W. H. Chiang, Y. S. Li, G. L. Chen, Y. A. Leu, T. C. Tien, S. C. Lo, L. Y. Lin, J. J. Lin and K. C. Ho, *Sens. Actuators, B: Chem.*, 2017, 248, 288-297.
37. D. Yuan, Z. Wei, P. Han, C. Yang, L. Huang, Z. Gu, Y. Ding, J. Ma and G. Zheng, *J. Mater. Chem., A*, 2019, 7, 16979-16983.
38. J. Xie, X. Zhao, M. Wu, Q. Li, Y. Wang and J. Yao, *Angew. Chem. Int. Ed.*, 2018, 57, 9640-9644.
39. W. Li, M. Seredych, E. Rodriguez-Castellon and T. J. Bandosz, *ChemSusChem*, 2016, 9, 606-616.
40. N. Sreekanth, M. A. Nazrulla, T. V. Vineesh, K. Sailaja and K. L. Phani, *Chem. Commun.*, 2015, 51, 16061-16064.
41. H. Yang, Y. Wu, Q. Lin, L. Fan, X. Chai, Q. Zhang, J. Liu, C. He and Z. Lin, *Angew. Chem. Int. Ed.*, 2018, 57, 15476-15480.
42. F. Pan, B. Li, W. Deng, Z. Du, Y. Gang, G. Wang and Y. Li, *Appl. Catal. B-Environ.*, 2019, 252, 240-249.
43. R. Wang, X. Sun, S. Ould-Chikh, D. Osadchii, F. Bai, F. Kapteijn and J. Gascon, *ACS Appl. Mater. Interfaces*, 2018, 10, 14751-14758.
44. J. Xu, Y. Kan, R. Huang, B. Zhang, B. Wang, K.-H. Wu, Y. Lin, X. Sun, Q. Li, G. Centi and D. Su, *Carbon*, 2016, 9, 1085-1089
45. Q. Cheng, K. Mao, L. Ma, L. Yang, L. Zou, Z. Zou, Z. Hu and H. Yang, *ACS Energy Lett.*, 2018, 3, 1205-1211.
46. .D. M. Feng, Y. P. Zhu, P. Chen and T. Y. Ma, *Catalysts*, 2017, 7, 373.
47. J. Hao and W. Shi, *Chin. J. Catal.*, 2018, 39, 1157-1166.
48. M. Jia, Q. Fan, S. Liu, J. Qiu and Z. Sun, *Curr. Opin. Green Sustain. Chem.*, 2019, 16, 1-6.
49. T. Wang, Q. Zhao, Y. Fu, C. Lei, B. Yang, Z. Li, L. Lei, G. Wu and Y. Hou, *Small Methods*, 2019, 1900210.
50. C. Lei, H. Chen, J. Cao, J. Yang, M. Qiu, Y. Xia, C. Yuan, B. Yang, Z. Li, X. Zhang, L. Lei, J. Abbott, Y. Zhong, X. Xia, G. Wu, Q. He and Y. Hou, *Adv. Energy Mater.*, 2018, 8, 1801912.
51. C. Lu, J. Yang, S. Wei, S. Bi, Y. Xia, M. Chen, Y. Hou, M. Qiu, C. Yuan, Y. Su, F. Zhang, H. Liang and X. Zhuang, *Adv. Funct. Mater.*, 2019, 29, 1806884.
52. A. S. Varela, W. Ju, A. Bagger, P. Franco, J. Rossmeisl and P. Strasser, *ACS Catal.*, 2019, 9, 7270-7284.
53. K. Wu, X. Chen, S. Liu, Y. Pan, W.-C. Cheong, W. Zhu, X. Cao, R. Shen, W. Chen, J. Luo, W. Yan, L. Zheng, Z. Chen, D. Wang, Q. Peng, C. Chen and Y. Li, *Nano Res.*, 2018, 11, 6260-6269.
54. H. B. Yang, S.-F. Hung, S. Liu, K. Yuan, S. Miao, L. Zhang, X. Huang, H.-Y. Wang, W. Cai, R. Chen, J. Gao, X. Yang, W. Chen, Y. Huang, H. M. Chen, C. M. Li, T. Zhang and B. Liu, *Nat. Energy*, 2018, 3, 140-147.
55. P. Su, K. Iwase, S. Nakanishi, K. Hashimoto and K. Kamiya, *Small*, 2016, 12, 6083-6089.
56. C. Yan, H. Li, Y. Ye, H. Wu, F. Cai, R. Si, J. Xiao, S. Miao, S. Xie, F. Yang, Y. Li, G. Wang and X. Bao, *Energy Environ. Sci.*, 2018, 1204-121048.
57. X. Li, W. Bi, M. Chen, Y. Sun, H. Ju, W. Yan, J. Zhu, X. Wu, W. Chu, C. Wu and Y. Xie, *J. Am. Chem. Soc.*, 2017, 139, 14889-14892.
58. T. Möller, W. Ju, A. Bagger, X. Wang, F. Luo, T. Ngo Thanh, A. S. Varela, J. Rossmeisl and P. Strasser, *Energy Environ. Sci.*, 2019, 12, 640-647.
59. J. Gu, C.-S. Hsu, L. Bai, H. M. Chen and X. Hu, *J. Am. Chem. Soc.* 2019, 364, 1091-1094.
60. Y. Pan, R. Lin, Y. Chen, S. Liu, W. Zhu, X. Cao, W. Chen, K. Wu, W.-C. M. Cheong, Y. Wang, L. Zheng, J. Luo, Y. Lin, Y. Liu, C. Liu, J. Li, Q. Lu, X. Chen, D. Wang and Y. Li, *J. Am. Chem. Soc.* 2018, 140, 4218-4221.
61. B. Zhang, J. Zhang, J. Shi, D. Tan, L. Liu, F. Zhang, C. Lu, Z. Su, X. Tan, X. Cheng, B. Han, L. Zheng and J. Zhang, *Nat. Commun.*, 2019, 10, 2980.
62. K. Jiang, S. Siahrostami, A. J. Akey, Y. Li, Z. Lu, J. Lattimer, Y. Hu, C. Stokes, M. Gangishetty, G. Chen, Y. Zhou, W. Hill, W.-B. Cai, D. Bell, K. Chan, J. K. Nørskov, Y. Cui and H. Wang, *Chem,* 2017, 3, 950-960.
63. Y. Hou, M. Qiu, M. G. Kim, P. Liu, G. Nam, T. Zhang, X. Zhuang, B. Yang, J. Cho, M. Chen, C. Yuan, L. Lei and X. Feng, *Nat. Commun.*, 2019, 10, 1392.
64. F. Pan, A. Liang, Y. Duan, Q. Liu, J. Zhang and Y. Li, *J. Mater. Chem., A*, 2017, 5, 13104-13111.
65. B. Dembinska, W. Kicinski, A. Januszewska, A. Dobrzeniecka and P. J. Kulesza, *J. Electrochem. Soc.*, 2017, 164, H484-H490.
66. S. Perez-Rodriguez, E. Pastor and M. J. Lazaro, *J. CO_2 Util.*, 2017, 18, 41-52.
67. M. N. Hossain, J. Wen and A. Chen, *Sci. Rep.*, 2017, 7, 1-10.
68. C. Z. Yuan, H. B. Li, Y. F. Jiang, K. Liang, S. J. Zhao, X. X. Fang, L. B.

Ma, T. Zhao, C. Lin and A. W. Xu, *J. Mater. Chem., A*, 2019, 7, 6894-6900.
69. Y. X. Duan, F. L. Meng, K. H. Liu, S. S. Yi, S. J. Li, J. M. Yan and Q. Jiang, *Adv. Mater.*, 2018, 30, 1706194.
70. C. Lei, Y. Wang, Y. Hou, P. Liu, J. Yang, T. Zhang, X. Zhuang, M. Chen, B. Yang, L. Lei, C. Yuan, M. Qiu and X. Feng, *Energy Environ. Sci.*, 2019, 12, 149-156.
71. M. Jia, C. Choi, T. S. Wu, C. Ma, P. Kang, H. Tao, Q. Fan, S. Hong, S. Liu, Y. L. Soo, Y. Jung, J. Qiu and Z. Sun, *Chem. Sci.*, 2018, 9, 8775-8780.
72. S. M. Bashir, S. S. Hossain, S. ur Rahman, S. Ahmed and M. M. Hossain, *Electrocatalysis*, 2015, 6, 544-553.
73. P. Sekar, L. Calvillo, C. Tubaro, M. Baron, A. Pokle, F. Carraro, A. Martucci and S. Agnoli, *ACS Catal.*, 2017, 7695-7703.
74. F. Li, S.-F. Zhao, L. Chen, A. Khan, D. R. MacFarlane and J. Zhang, *Energy Environ. Sci.*, 2016, 9,216-223.
75. X. Lu, T. H. Tan, Y. H. Ng and R. Amal, *Chem. Eur. J.*, 2016, 22, 11991-11996.
76. H. M. Jhong, C. E. Tornow, B. Smid, A. A. Gewirth, S. M. Lyth and P. J. Kenis, *ChemSusChem*, 2017, 10, 1094-1099.
77. S. Guo, S. Zhao, X. Wu, H. Li, Y. Zhou, C. Zhu, N. Yang, X. Jiang, J. Gao, L. Bai, Y. Liu, Y. Lifshitz, S.-T. Lee and Z. Kang, *Nat. Commun.*, 2017, 8, 1828.
78. J. Liu, C. Guo, A. Vasileff and S. Qiao, *Small Methods*, 2017, 1, 1600006.
79. K. Jiang, S. Siahrostami, T. Zheng, Y. Hu, S. Hwang, E. Stavitski, Y. Peng, J. J. Dynes, M. Gangishetty, D. Su, K. Attenkofer and H. Wang, *Energy Environ. Sci.*, 2018, 11, 893-903.
80. T. Zheng, K. Jiang, N. Ta, Y. Hu, J. Zeng, J. Liu and H. Wang, *Joule*, 2019, 3, 265-278.Pan, B. Li, W. Deng, Z. Du, Y. Gang, G. Wang and Y. Li, *Appl. Catal. B: Environ.*, 2019, 252, 240-249.
81. Y. Cheng, S. Zhao, B. Johannessen, J.-P. Veder, M. Saunders, M. R. Rowles, M. Cheng, C. Liu, M. F. Chisholm, R. De Marco, H.-M. Cheng, S.-Z. Yang and S. P. Jiang, *Adv. Mater.*, 2018, 30, 1706287.
82. Z. Zhang, C. Ma, Y. Tu, R. Si, J. Wei, S. Zhang, Z. Wang, J.-F. Li, Y. Wang and D. Deng, *Nano Res.*, 2019, DOI: 10.1007/s12274-019-2316-2319.
83. X. Qin, S. Zhu, F. Xiao, L. Zhang and M. Shao, *ACS Energy Lett.*, 2019, 4, 1778-1783.
84. T. N. Huan, N. Ranjbar, G. Rousse, M. Sougrati, A. Zitolo, V. Mougel, F. Jaouen and M. Fontecave, *ACS Catal.*, 2017, 7, 1520-1525.
85. C. Zhang, S. Yang, J. Wu, M. Liu, S. Yazdi, M. Ren, J. Sha, J. Zhong, K. Nie, A. S. Jalilov, Z. Li, H. Li, B. I. Yakobson, Q. Wu, E. Ringe, H. Xu, P. M. Ajayan and J. M. Tour, *Adv. Energy Mater.*, 2018, 8, 1703487.
86. F. Yang, P. Song, X. Liu, B. Mei, W. Xing, Z. Jiang, L. Gu and W. Xu, *Electrocatalysis*, 2018, 57, 12303-12307.
87. Z. Chen, K. Mou, S. Yao and L. Liu, *Angew. Chem. Int. Ed.*, 2018, 11, 2944-2952.
88. W. Zheng, C. Guo, J. Yang, F. He, B. Yang, Z. Li, L. Lei, J. Xiao, G. Wu and Y. Hou, *Carbon*, 2019, 150, 52-59.
89. E. L. Clark, J. Resasco, A. Landers, J. Lin, L.-T. Chung, A. Walton, C. Hahn, T. F. Jaramillo and A. T. Bell, *ACS Catal.*, 2018, 8, 6560-6570.
90. J. G. Chen, C. W. Jones, S. Linic and V. R. Stamenkovic, *ACS Catal.*, 2017, 7, 6392-6393.